An auristatin-based antibody-drug conjugate targeting HER3 enhances the radiation response in pancreatic cancer

Laura Bourillon, Céline Bourgier, Nadège Gaborit, Véronique Garambois, Eva Lles, Alexandre Zampieri, Charline Ogier, Marta Jarlier, Nina Radosevic-Robin, Béatrice Orsetti, et al.

An auristatin-based antibody-drug conjugate targeting HER3 enhances the radiation response in pancreatic cancer

Laura Bourillon[1], Céline Bourgier[1,2], Nadège Gaborit[1], Véronique Garambois[1], Eva Llès[1], Alexandre Zampieri[1], Charline Ogier[1], Marta Jarlier[2], Nina Radosevic-Robin[3], Béatrice Orsetti[1], Hélène Delpech[1], Charles Theillet[1], Pierre-Emmanuel Colombo[1,2], David Azria[1,2], André Pèlegrin[1], Christel Larbouret[1,#], Thierry Chardès[1,4,#]

[1]Institut de Recherche en Cancérologie de Montpellier (IRCM), INSERM U1194, Université de Montpellier, Institut régional du Cancer de Montpellier (ICM), Montpellier, 34298, France

[2]Institut régional du Cancer de Montpellier (ICM), Montpellier, 34298, France

[3]Department of Biopathology, Jean Perrin Comprehensive Cancer Center and INSERM/UCA UMR 1240, Clermont-Ferrand, 63011, France

[4]Centre National de la Recherche Scientifique (CNRS)

# C. Larbouret and T. Chardès contributed equally to this work

Short title

HER3-ADC-mediated radiosensitization

Keywords

HER3/ErbB3, monomethylauristatin, irradiation, ADC, pancreatic cancer

Abbreviations: ADC: antibody-drug conjugate; BSA: bovine serum albumin ; CAFs: cancer-associated fibroblasts; DSB: double-strand break; ESMO: european society for medical oncology; FCS: fetal calf serum; FOLFIRINOX: fluorouracil-leucovorin-irinotecan-oxaliplatin; Gy: gray; HIC-HPLC: hydrophobic interaction chromatography-high performance liquid

chromatography; IR: irradiation; mAb: monoclonal antibody; MMAE: monomethyl auristatin E; NRG1: neuregulin 1; NSCLC: non-small cell lung carcinoma; PBS: phosphate-buffered saline; PDAC: pancreatic ductal adenocarcinoma; PDX: patient-derived xenograft; PI: propidium iodide; SSB: single-strand break; 7-AAD: 7-amino actinomycin D

Conflict of interest: N. Gaborit, A. Pèlegrin, C. Larbouret and T. Chardès are inventors of the WO2012/156532 patent "Anti-human HER3 and uses thereof", the WO2015/067986 patent "Neuregulin allosteric anti-HER3 antibody", and the WO2016/177664 patent "Low-fucose anti-human HER3 antibodies and uses thereof". The other authors declare no conflict of interest.

Article category: Cancer therapy and prevention

Financial support

This work was supported by the program "Investissement d'Avenir" (grant agreement: Labex MabImprove, ANR-10-LABX-53-01; A. Pèlegrin), by INSERM Transfert (CoPoC grant HER3ADC; T. Chardès) and the SIRIC Montpellier Cancer (SIRIC Montpellier Cancer Grant INCa_Inserm_DGOS_12553; T. Chardès).

Corresponding author

Dr T. Chardès, Institut de Recherche en Cancérologie de Montpellier, Montpellier, 34298, France

e-mail : thierry.chardes@inserm.fr

Phone number: (33) 467 612 404

Fax number: (33) 467 613 727

Novelty and impact

In PDAC, chemoradiation is prescribed to patients with borderline resectable lesions, with the aim of reducing the tumor size to make surgery possible. The HER3 receptor is a key signaling hub in PDAC. We developed a novel antibody-drug conjugate targeting HER3 (HER3-ADC), which enhanced radiosensitivity of PDAC by arresting cells in G2/M. HER3-ADC increased the radiation response in mice xenografted with PDAC cells, through inhibition of survival, and induction of DNA break formation and apoptosis. The HER3-ADC plus irradiation combination would plausibly help to increase the rate of resection for patients with borderline resectable pancreatic cancer.

Abstract

Pancreatic ductal adenocarcinoma (PDAC) is an aggressive cancer characterized by poor response to chemo- and radiotherapy due to the lack of efficient therapeutic tools and early diagnostic markers. We previously generated the non-ligand competing anti-HER3 antibody 9F7-F11 that binds to pancreatic tumor cells and induces tumor regression *in vivo* in experimental models. Here, we asked whether coupling 9F7-F11 with a radiosensitizer, such as monomethylauristatin E (MMAE), by using the antibody-drug conjugate (ADC) technology could improve radiation therapy efficacy in PDAC. We found that the MMAE-based HER3 antibody-drug conjugate (HER3-ADC) was efficiently internalized in tumor cells, increased the fraction of cells arrested in G2/M, which is the most radiosensitive phase of the cell cycle, and promoted programmed cell death of irradiated HER3-positive pancreatic cancer cells (BxPC3 and HPAC cell lines). HER3-ADC decreased the clonogenic survival of irradiated cells by increasing DNA double-strand break formation (based on γH2AX level), and by modulating DNA damage repair. Tumor radiosensitization with HER3-ADC favored the inhibition of the AKT-induced survival pathway, together with more efficient caspase 3/PARP-mediated apoptosis. Incubation with HER3-ADC before irradiation synergistically reduced the phosphorylation of STAT3, which is involved in chemoradiation resistance. *In vivo*, the combination of HER3-ADC with radiation therapy increased the overall survival of mice harboring BxPC3, HPAC cell xenografts or patient-derived xenografts, and reduced proliferation (KI67-positive cells). Combining auristatin radiosensitizer delivery via an HER3-ADC with radiotherapy is a new promising therapeutic strategy in PDAC.

Introduction

Approximately 50-60% of all patients with cancer receive radiation treatment the efficacy of which is sometimes limited by radiation toxicities and tumor radioresistance. For instance, in pancreatic ductal adenocarcinoma (PDAC), chemoradiation is prescribed to patients with borderline resectable lesions, with the aim of reducing the tumor size and improving the feasibility of complete resection with free microscopic surgical margins (R0). Radiotherapy combined with chemotherapy may also be proposed for treatment of non-metastatic locally advanced disease (ESMO guidelines) [1]. Nevertheless, PDAC remains one of the most aggressive tumors with an extremely poor prognosis (survival rate of 6 months) and is expected to become the second leading cause of cancer-related death by 2030 [2]. This dramatic outcome is related to the lack of efficient therapeutic tools, early diagnostic markers, and high resistance to chemo and radiotherapy [3].

Reducing tumor radioresistance, limiting the exposure of the surrounding normal tissues, and improving tumor control are the major goals to improve radiotherapy efficiency in cancer. Free payloads used in the antibody-drug conjugate (ADC) technology, such as maytansinoids or auristatins, are efficient radiosensitizers [4,5], but with high off-target side effects. ADCs that target EGFR or HER2 efficiently radiosensitize esophageal, gastric, head and neck tumor cells [5]. However, clinical trials that tested the combination of anti-EGFR or HER2 antibodies with gemcitabine for patients with pancreatic cancer did not find any additional benefit compared with gemcitabine alone [6,7], thus limiting the use of such antibodies for ADC-induced radiosensitization in PDAC. Moreover, ADCs derived from anti-EGFR or -HER2 antibodies should be used with caution due to the skin and heart toxicities observed with the naked antibodies.

The HER3 receptor is a key signaling hub in PDAC. HER3 expression correlates with tumor progression and reduced PDAC patient survival [8]. HER3 is one of the main actors of acquired resistance to EGFR- and HER2-targeted therapies through activation of a compensatory PI3K/AKT survival pathway [9,10], and antagonizes tumor growth inhibition by

insulin-like growth factor receptor (IGFR) inhibitors [11]. The HER3 ligand neuregulin (NRG1) has been characterized as the dominant activator of the PI3K/AKT pathway in PDAC [12]. Cancer-associated fibroblasts (CAFs) from the pancreatic tumor stroma secrete NRG1 to promote cancer cell proliferation by HER3/AKT signaling activation [13]. Moreover, the HER3/AKT/Src axis contributes to cancer cell survival following radiation therapy [14–16], showing that HER3 is a critical radiation regulator, particularly in PDAC [17].

We previously generated the non-NRG1 competing allosteric anti-HER3 antibody 9F7-F11 that binds to pancreatic tumor cells independently of neuregulin permeation [18]. It also blocks the PI3K/AKT pathway [19,20], and induces HER3 downregulation [21], leading to *in vivo* tumor regression. Here, we asked whether coupling 9F7-F11 with a radiosensitizer, such as monomethylauristatin E (MMAE), by using the ADC technology could improve radiation therapy in PDAC. We found that the MMAE-9F7-F11 ADC (HER3-ADC throughout the text) was efficiently internalized in BxPC3 and HPAC pancreatic tumor cells and induced cell cycle arrest in G2/M, the most radiosensitive phase of the cell cycle [22]. HER3-ADC enhanced their radiosensitivity by decreasing clonogenic survival and modulating the DNA damage response. HER3-ADC also limited the compensatory activation of pro-survival AKT signaling after irradiation, and favored apoptosis by increasing caspase-3 cleavage and PARP activation. *In vivo*, HER3-ADC increased tumor control by radiation therapy in mice harboring BxPC3 cell and patient-derived xenografts (PDX). Targeted delivery of a radiosensitizer through HER3-ADC could broaden the therapeutic window of radiation therapy in pancreatic cancer.

Materials and Methods

Cell culture

The BxPC3, HPAC, CFPAC-1, Capan-1 and MiaPaCa-2 human pancreatic cancer cell lines, the A549 human lung carcinoma and the MCF7 human breast adenocarcinoma cell lines were obtained from the American Type Culture Collection (Rockville, MD). The cell lines were mycoplasma-free, as determined using the MycoAlert™ Detection Kit (Lonza, Switzerland), and were authenticated by short tandem repeat profiling using the Promega PowerPlex 21 System. The PDX P4604 was obtained from a resected hepatic metastasis surgery sample from a patient with PDAC treated with gemcitabine. The PDX P4604 was cryopreserved after three *in vivo* passages in nude mice (PDX platform, Institut de Recherche en Cancérologie de Montpellier). The cell line P4604 was derived from the PDX P4604 after *in vitro* serial passages. BxPC3, Capan-1, A549 and MCF7 cells were grown in RPMI medium with 10% fetal calf serum (FCS) and antibiotics, whereas HPAC, CFPAC-1, MiaPaca-2 and P4604 cells were cultured in DMEM with 10% FCS and antibiotics.

Reagents

Recombinant human HER3 extracellular domain (ECD) and recombinant human NRG1 ECD were from R&D Systems (Minneapolis, MN). The mouse anti-HER3 monoclonal antibody (mAb) 9F7-F11 was obtained as previously described [19]. The control antibody 12G4 is an anti-Müllerian Inhibiting Substance mAb. For western blotting, rabbit and mouse mAbs against proteins involved in DNA damage repair [phosphorylated (p-)ATM, p-CHK2, p-ATR, p-CHK1, p-NBS1, MRE11, RAD50, p-BRCA1, and DNA-PK), survival (p-HER3, p-AKT, STAT3 and p-STAT3), and apoptosis (cleaved caspase 3, cleaved PARP, p-BAD and BAD) were from Cell Signaling Technology (Danvers, MA).

Generation of the MMAE-based anti-HER3 antibody-drug conjugate (HER3-ADC)

HER3-ADC was synthesized and characterized by Levena Biopharma (San Diego, CA). 9F7-F11 [19] was conjugated via the protease-sensitive linker maleimidocaproyl-valine-citrulline-*p*-aminobenzyloxycarbonyl to MMAE (MC-vc-PAB-MMAE) using the Seattle Genetics method [23] (patent US 7659241). The mean Drug to Antibody Ratio was determined by Hydrophobic Interaction Chromatography-High Performance Liquid Chromatography (HIC-HPLC) based on the SH/Ab ratio, and ranged between 3.4 and 4.3. HIC-HPLC analysis was performed on a Tosoh TSKgel Butyl-NPR column, with buffer A (20mM sodium phosphate, 1.5M ammonium sulfate, pH7.0) and buffer B (20mM sodium phosphate, 25% v/v isopropanol, pH 7.0), and an Agilent HPLC system. High-molecular aggregates were less than 2% in all preparations, as characterized by size-exclusion chromatography performed on a Tosoh TSKgel G3000SW-XL column, with buffer containing 150mM sodium phosphate and 300mM sodium chloride, pH7.0, and an Agilent 1100 HPLC system. The level of free MMAE was below 1%, as determined by reverse phase chromatography on a Zorbax Eclipse XDB-C18 column, with buffer A (0.05% trifluoroacetic acid in water) and buffer B (0.045% trifluoroacetic acid in acetonitrile).

Irradiation procedure

Cells were irradiated with a linear particle accelerator (Varian Medical Systems; Palo Alto, CA) at the Radiotherapy Department of the ICM hospital. Radiation was delivered as a single dose of 6MV-photons (2 to 4 Gy) in a 40cm × 40cm field size at a dose rate of 200UM/min. For *in vivo* experiments, radiation was delivered to the flank of anesthetized mice simultaneously in a 2cm x 2cm field size at dose rate of 400 UM/min (source-half depth distance, 100 cm).

HER3 binding assessment by ELISA

Flat-bottom 96-well Maxisorp plates (Nunc, Paisley, UK) were coated with 25ng/well of recombinant human HER3 ECD at 4°C for 18h, and then blocked with 1% bovine serum

albumin (BSA) in phosphate-buffered saline (PBS) containing 0.1% Tween 20 (PBS-T). After washes in PBS-T, ten-fold dilutions of 9F7-F11 and HER3-ADC were added at 37°C for 2h. After washes with PBS-T, antibody binding to HER3 was detected by incubation with a peroxidase-conjugated goat $F(ab')_2$ antibody against mouse $F(ab')_2$ (Jackson Immunoresearch, West Grove, PA) at 37°C for 1h. After three washes with PBS-T, 3,3,5,5 tetramethylbenzidine (Sigma, St Louis, MO) was used for detecting peroxidase activity before addition of 1M H_2SO_4 to stop the reaction. Absorbance was measured at 450 nm.

Analysis of HER3-ADC internalization by immunofluorescence

For each assay, $3x10^4$ cells were plated on coverslips in a 24-well plate. Two days later, during the logarithmic phase of growth, cells were incubated with 50 µg/mL of 9F7-F11 or HER3-ADC labeled with FITC (FluoProbes® 488, Interchim; France) at 4°C or 37°C for various times. Cells were then washed twice with PBS and 1mg/ml BSA (PBS-BSA), and once with PBS. After fixation in formalin (3.7% *p*-formaldehyde in PBS) for 40min, cells were permeabilized with 0.5% Triton X-100/PBS for 15min. Cells were washed twice with PBS-BSA and incubated in PBS-BSA for 40min. After three washes with PBS, coverslips were mounted with Vectashield® with DAPI (Vector Laboratories, Burlingame, CA) and cells were visualized using an epifluorescence Zeiss Imager 2 (Zeiss, Germany).

Cell viability assay

Cells were plated in 96-well flat-bottom plates the day before starvation in 1% FCS for 24h. HER3-ADC at different dilutions was then added for 5 days, with 50ng/ml NRG1. In absence of NRG1 stimulation, cells were maintained in 10% FCS and treated with HER3-ADC. Cell viability was then measured using the CellTiter 96 Aqueous One Solution Cell Proliferation Assay (Promega, Madison, WI). Colorimetry was measured at 490 nm absorbance. All experiments were done in triplicate.

Clonogenic survival

After trypsinization, cells were seeded in triplicate in 6-well plates and were incubated with HER3-ADC (different concentrations) in complete medium, 24h before irradiation (2Gy). At 10 to 14 days post-irradiation, cells were fixed with 1:3 acetic acid/methanol solution and stained with Giemsa in water (3.5:10) (Sigma-Aldrich, St Louis, MO). Colonies containing at least 50 cells were counted, and the surviving fraction was calculated as the fraction of surviving cells relative to untreated cells. All experiments were performed in duplicate.

Cell cycle analysis

After 24h-serum starvation (1% FCS), cells were incubated with various concentrations of HER3-ADC or 9F7-F11 together with 50ng/ml NRG1 for different time points before cell cycle analysis. Alternatively, 1 μg/ml HER3-ADC was added 24h before irradiation (2Gy), and cell cycle was analyzed 24h after radiation exposure. In each experiment, cells were then fixed in 75% ethanol at 4°C for 10min, and then incubated with 100 μg/ml RNase (Qiagen, Hilden, Germany). After staining with 40 μg/ml propidium iodide (PI) (Sigma-Aldrich), cell cycle was analyzed with a Gallios flow cytometer using the Kaluza analysis software (Beckman Coulter, Brea, CA). All experiments were done in triplicate.

AnnexinV/7-AAD measurement by flow cytometry

After 24h-serum starvation (1% FCS), cells were co-incubated with 50ng/ml NRG1 and various concentrations of HER3-ADC or 9F7-F11 for 24h, before irradiation (4Gy). Apoptosis was measured 48h after irradiation using the Annexin-V/7-AAD Detection Kit (Beckman Coulter), according to the manufacturer's instructions. After PBS washes, cells were incubated with 10μl AnnexinV-FITC and 20μl 7-Amino Actinomycin D (7-AAD) at room temperature (RT) in the dark for 15min. Data were acquired on a Gallios flow cytometer and analyzed with the Kaluza software (Beckman Coulter). All experiments were performed in duplicate.

Tumor xenografts and treatment

All *in vivo* experiments were performed in compliance with the French regulations and ethical guidelines for experimental animal studies in an accredited establishment (Agreement No. C34-172-27). BxPC3 ($3.5x10^6$), HPAC ($3.5x10^6$) and P4604 ($8x10^6$) cells were subcutaneously injected in the right flank of six-week-old female athymic nude Hsd mice (Envigo; Huntingdon, UK). Tumor-bearing mice were randomized to different treatment groups (at least six animals/group) when tumors reached a volume of 100 mm^3. Animals bearing BxPC3 and HPAC cell xenografts received 2 mg/kg of HER3-ADC by intraperitoneal injection twice per week for 4 weeks (Q3D-4W). Fractionated irradiation (4Gy) was performed 24h after each injection. Mice with P4604 xenografts received one single intravenous injection of 5 mg/kg of HER3-ADC before one single 8Gy fraction 24h later. Tumor volumes were calculated by using the formula: $D_1 \times D_2 \times D_3 /2$. For survival analyses, mice were sacrificed when tumors reached a volume of 1000 mm^3.

Immunofluorescence analysis of γH2AX expression

Cells were seeded at a density of 2×10^4 cells/ml on coverslips in 24-well plates, and serum-starved for 24h. Cells were then co-incubated with 50ng/ml NRG1 and 5μg/ml HER3-ADC or 9F7F11, before irradiation (2Gy) 24h later. At 30min post-irradiation, cells were rinsed with PBS, fixed in 4% formaldehyde at RT for 20min, and then washed with PBS. Cells were permeabilized in 0.5% Triton-X100 in PBS at RT for 15min. After two PBS washes, non-specific binding was blocked by incubation with PBS-BSA at 37°C for 30min. Cells were then incubated with an anti–γH2AX (Ser139) antibody (1:200 in PBS-BSA; Millipore, Burlington, MA) at 37°C for 1h. After 3 washes in PBS-T, cells were incubated with an anti-mouse immunoglobulin G antibody-FITC conjugate (1:400 in PBS-BSA; Millipore) at 37°C for 40min. After three washes in PBS-T, coverslips were mounted with Vectashield with DAPI, and γH2AX foci were visualized using an epifluorescence Zeiss Imager 2 (Oberkochen, Germany).

Immunohistochemistry

Immunohistochemistry (IHC) analysis of formalin-fixed, paraffin-embedded (FFPE) tissue sections from tumor xenografts was performed as described previously [20,24]. Quantification was done with the Image Scope software. Surgically excised, human FFPE PDAC specimens were cut into 4-µm sections that were deparaffinized in xylene and hydrated in graded alcohols. Antigen retrieval was performed at 97°C for 20 min in EnVision® Target Retrieval Solution High pH (Dako, Glostrup, Denmark). Sections were then incubated at 37°C with mouse monoclonal anti-HER3 (clone DAK-H3-IC, Dako) or mouse anti-Neuregulin (clone 7D5, Novus Biologicals, Littleton) antibodies diluted at 1:50 for 2h. The antigen-antibody reaction was revealed using EnVision® Flex DAB System in a Dako Autostainer Plus automate. IHC staining was interpreted by an expert pathologist who was blind to patient information.

Phosphokinome and stress/apoptosis signalosome

After serum starvation for 24h, BxPC3 cells were incubated with 1µg/ml HER3-ADC and 50ng/ml NRG1 for 24h, prior to irradiation (2Gy). Cell lysates, prepared 60min later, were used to determine: i) the relative phosphorylation levels of 43 kinases with the Human Phospho-Kinase Array kit (RD Systems, Minneapolis, MN); ii) the expression levels of 35 apoptosis-related proteins with the Human Apoptosis Antibody Array kit (RD Systems); and iii) the expression levels of 19 signaling molecules involved in the regulation of the stress response and apoptosis with the Human Stress and Apoptosis Signaling Antibody Array kit (Cell Signaling Technology). Expression levels were determined by quantification with the ImageJ software.

Electrophoresis and western blotting

After serum starvation for 24h and washes in PBS, cells were co-incubated with 50ng/ml NRG1 and 1µg/ml HER3-ADC, before irradiation (2Gy) 24h later. At 60min and 24h post-irradiation, cells were washed, scraped and lysed with lysis buffer [20mM Tris-HCl pH 7.5,

150mM NaCl, 1.5mM $MgCl_2$, 1mM EDTA, 1% Triton X-100, 10% glycerol, 0.1mM phenylmethylsulfonyl fluoride, 100mM sodium fluoride, 1mM sodium orthovanadate (Sigma), and one tablet of complete protease inhibitor mixture (Roche Diagnostics, Indianapolis, IN)]. After 30min, the insoluble fraction was cleared by centrifugation and protein concentration in cell lysates was determined with the Bradford assay. After SDS-PAGE electrophoresis in reducing conditions, proteins were transferred to polyvinylidene difluoride membranes (GE Healthcare, Little Chalfont, UK) that were then saturated in PBS-T with 5% nonfat dry milk at 25°C for 1h. Membranes were incubated with primary antibodies diluted in PBS-T/5% BSA at 4°C for 18h. After three washes in PBS-T, the appropriate peroxidase-conjugated secondary antibodies (Sigma) were added in PBS-T/5% nonfat dry milk at 25°C for 1h. After three washes in PBS-T, blots were visualized using a chemiluminescent substrate (Western lightning Plus-ECL, PerkinElmer, Waltham, MA; or Super Signal West Femto Substrate, ThermoFisher Scientific, Waltham, MA).

Statistical Analysis

Statistical analysis of *in vivo* data was performed using the STATA 11.0 software (StataCorp., College Station, TX) as previously described [19]. Statistical analysis of the *in vitro* results was done with GraphPad Prism 6 (San Diego, CA) using one-way ANOVA followed by the Dunnett's test (comparison with untreated cells).

Results

HER3-ADC is internalized and inhibits viability of pancreatic cancer cells

We initially checked that HER3-ADC binds to and is internalized in tumor cells. ELISA assays showed that like the naked antibody 9F7-F11, HER3-ADC bound to HER3 in a dose-dependent manner, with a half-maximal effective concentration (EC_{50}) of 1.98±0.74 ng/ml (9F7-F11: EC_{50}=1.93±0.96 ng/ml) (Fig. 1A). Microscopy monitoring of fluorescein-labeled HER3-ADC internalization in MCF7 cells at 4°C and 37°C (Fig.1B) showed that at 10min, fluorescence was localized at the cell surface. At 4°C, fluorescein-labeled HER3-ADC remained at the cell membrane throughout the experiment. Conversely, at 37°C, we detected small intracellular patches of fluorescein-labeled HER3-ADC already at 30min post-binding and up to 120min, demonstrating HER3-ADC internalization in tumor cells. HER3-ADC internalization was comparable to that of fluorescein-conjugated 9F7-F11 (Supplementary Fig. S1). We then tested HER3-ADC effect on the viability of the pancreatic cancer cell lines BxPC3 and HPAC, and the PDX cell line P4604. These three cell lines express HER3 at comparable levels (Supplementary Fig. S2). HER3-ADC (1 to 5μg/ml) inhibited BxPC3, HPAC and P4604 cell viability in a dose-dependent manner, particularly after stimulation with recombinant NRG1 (Fig. 1C; NRG1-stimulated cells) to mimic NRG1 paracrine secretion by stromal CAFs. At the highest HER3-ADC concentration, viability was inhibited by 90% in stimulated BxPC3 cells, and by 30% and 25% in stimulated HPAC and P4604 cells, respectively. Naked 9F7-F11 was less efficient at the 1-5μg/ml concentration range we used in this experiment, although previously showing efficacy at higher doses[18,19], and the negative antibody control did not affect cell viability (Fig.1C). No effect on cell viability was also observed on HER3-negative pancreatic cancer cells Capan-1 and MiaPaCa-2 (Supplementary Fig.S3). Finally, clonogenic survival of BxPC3 and HPAC cells was reduced by HER3-ADC in a dose-dependent manner (Fig.1D).

HER3-ADC induces pancreatic cancer cell cycle arrest in the G2/M phase

To examine HER3-ADC effects on the cell cycle and apoptosis, we incubated serum-starved BxPC3 cells with NRG1 and various concentrations of HER3-ADC. At different time points (0.5h to 48h), we stained cells with PI to analyze the cell cycle (Supplementary Fig.S4A), or with annexin V/7-AAD to discriminate between early and late apoptotic cells (Supplementary Fig.S4B). Incubation with HER3-ADC, but not with medium alone or 9F7-F11, resulted in a time-dependent increase of G2/M-arrested cells (Fig.2A). At 24h-post exposure, 49% of cells incubated with 5μg/ml HER3-ADC were in the G2/M phase, compared with 19% of cells incubated with 5μg/ml 9F7-F11 (Fig.2B). Conversely, 9F7-F11 promoted accumulation of BxPC3 cells in the G1 phase, as previously reported [19]. HER3-ADC promoted accumulation in G2/M also of HPAC cells (data not shown). At 24h, the sub-G1 DNA content (an indicator of apoptosis-related DNA fragmentation) was also increased in HER3-ADC-treated BxPC3 cells compared with medium- or 9F7-F11-treated cells (Fig.2C). In agreement, the percentage of early (annexin V-positive/7-ADD-negative) and late (annexin V-positive/7-ADD-positive) apoptotic cells at 48h post-exposure was higher in HER3-ADC-treated than in medium- or 9F7-F11-treated cells (Fig.2D). These data suggest that in pancreatic cancer cells, HER3-ADC induces cell cycle arrest in the G2/M phase and promotes apoptosis.

HER3-ADC enhances radiosensitivity of pancreatic cancer cells

As HER3-ADC promotes arrest in G2/M, the most radiosensitive phase of the cell cycle, we next investigated whether HER3-ADC increases pancreatic cancer cell radiation response by analyzing the clonogenic survival of BxPC3, HPAC and P4604 cells. At day 14 post-treatment, the number of Giemsa-stained colonies was much lower in cells incubated with 2 or 5μg/ml HER3-ADC 24h before irradiation (2Gy) than in cultures incubated with HER3-ADC alone or only irradiated (Fig.3A). This was confirmed by quantification of ethanol solubilized blue colonies (Fig.3B), and by measurement of the surviving fraction of BxPC3 cells exposed to medium, radiation (2Gy) or/and HER3-ADC (Supplementary Fig.S5). These results

demonstrated that HER3-ADC enhances pancreatic tumor cell radiosensitivity. In contrast, naked 9F7-F11, at dose of 100μg/ml, did not synergize with irradiation, as demonstrated by clonogenic survival of CFPAC-1 and HPAC cells (Supplementary Fig.S6).

HER3-ADC increases the radiation response in mice xenografted with pancreatic cancer cells and PDX cells

To determine whether HER3-ADC-induced radiosensitization could improve the response to radiation therapy *in vivo*, we treated mice xenografted with BxPC3 or HPAC cells with HER3-ADC (2mg/kg) and/or irradiation (4Gy) 24h after every HER3-ADC injection (Q3D-4W). The HER3-ADC+radiation therapy combination increased the median survival by 21 days and by 19 days in BxPC3 and HPAC cell-xenografted mice, respectively, compared with irradiation alone, and by 35 days and 44 days, respectively, compared with control (Fig.4A and 4B). We did not observe any weight loss during the experiment (data not shown), suggesting limited toxicity of the HER3-ADC+radiation combination. Similarly, in nude mice xenografted with the PDX P4604, the combined treatment (single dose of 8Gy of irradiation 24h after 5mg/kg HER3-ADC) increased the median survival by 30 days compared with irradiation alone, and by 41 days compared with control (Fig.4C). At 75 days post-treatment of P4604-xenografted mice, all mice treated with the HER3-ADC+irradiation combination were still alive, whereas most of the mice treated with radiation alone, and all control mice were dead (tumor volume = 1000mm^3). These results indicate that HER3-ADC efficiently promotes the radiation response in pancreatic tumor cell lines and PDX. Moreover, analysis of PDX P4604 samples at day 15 post-treatment (Fig.4D) showed that the number of cancer cells positive for KI67 (cell proliferation) (Fig.4E) and for cleaved caspase-3 (apoptosis) (Fig.4F) was reduced in mice treated with HER3-ADC+radiation compared with mice that were only irradiated.

As the 9F7-F11 antibody is more effective in the presence of NRG1 [18], we investigated by immunohistochemistry HER3 and NRG1 expression in tumor specimens from 45 patients with PDAC (Fig.4G). NRG1 and HER3 were expressed in 21 (46%) and 10 (22%) PDAC

samples, respectively, and co-expressed in 7 samples (15%) (Fig.4H), indicating that 70% of the HER3-positive PDAC samples were also NRG1-positive.

HER3-ADC increases DNA double-strand break formation in irradiated pancreatic cancer cells

To thoroughly investigate HER3-ADC effect on cell radiation response, we first characterized the radiation-induced DNA damage by examining γH2AX expression (a marker of DNA double-strand break formation) by flow cytometry after irradiation (2Gy). As exemplified in Fig.5A and quantified in Fig.5B, the number of γH2AX-positive BxPC3 cells measured by flow cytometry was significantly higher in cultures incubated with HER3-ADC 24h before irradiation compared with cultures exposed only to HER3-ADC ($p<0.01$) or irradiation ($p<0.1$) (Fig.5B). This was confirmed by immunofluorescence (Fig.5C) where quantification of γH2AX foci (Fig.5D) showed a significant increase in the number of γH2AX foci (up to 12±2) in BxPC3 cells incubated with HER3-ADC before irradiation compared with cells pre-incubated with medium or 9F7-F11 before irradiation (around 5.5±3 foci) ($p<0.001$) and with non-irradiated cells (between 2.5±1 and 5.5±2 foci) ($p<0.001$). Moreover, the percentage of irradiated BxPC3 cells with more than 15 γH2AX foci per nucleus (Fig.5E) was significantly increased after pre-incubation with HER3-ADC (around 35% cells) compared with all other conditions ($p<0.001$). These data indicate that HER3-ADC-induced radiosensitivity in pancreatic cancer cells can at least in part be explained by a significant increase of severe DNA damage.

HER3-ADC inhibits the radiation-induced survival pathway, and promotes the DNA damage response and apoptotic signaling

To better understand the molecular mechanisms underlying HER3-ADC-induced radiosensitivity we analyzed the phosphokinome and stress/apoptosis signalosome in NRG1-stimulated BxPC3 cells pre-incubated or not with HER3-ADC 24h before irradiation.

Irradiation alone induced the phosphorylation of different proteins involved in cell survival, proliferation and inflammation at 1h post-exposure (Fig. 6A). Pre-incubation with HER3-ADC reduced the irradiation-induced phosphorylation of some of these proteins, such as AKT, GSK3, AMPK, STAT family members, and β-catenin. Conversely, it increased the expression/activation of pro-apoptotic factors, such as the expression of death receptors DR4 and DR5, BAX and BAD, the cleavage of caspase 3 and PARP, and the phosphorylation of SMAD2 that favors TGFβ-induced apoptosis. Pre-incubation with HER3-ADC also reduced the expression levels of anti-apoptotic proteins, such as phosphorylated BAD, cleaved IAP1, XIAP and survivin, as well as of phosphorylated STAT3 and STAT5. The cellular response to radiation-induced DNA damage mainly involves the ATR/CHK1 and ATM/CHK2 pathways that are activated by DNA single-strand breaks (SSB) and double-strand breaks (DSB). Irradiation significantly increased the phosphorylation of the DNA damage checkpoint protein CHK2 (Fig. 6A). Pre-incubation with HER3-ADC did not affect the radiation-induced phosphorylation of CHK2, whereas it further reduced CHK1 phosphorylation. Finally, some positive or negative changes in expression/phosphorylation occurred early post-irradiation (0.5-1h) with a rapid return to baseline levels (e.g., p-p53, p-CHK2, p-SMAD2 and p-BAD) (Supplementary Fig.S7). Other radiation-induced changes (e.g., cleavage of caspase-3 and PARP, and CHK1 phosphorylation) progressed over time until 24h (end of the experiment), whereas other proteins (e.g., p-AKT, p-IκBα and IκBα) remained stable throughout the experiment. To confirm these results, we performed western blot analysis of cell lysates collected at 1h and 24h post-treatment (Fig.6B). Proteins involved in DSB DNA repair, such as p-ATM, p-CHK2, p-NBS1 and p-BRCA1, showed increased phosphorylation in response to irradiation, and also to HER3-ADC pre-incubation. Conversely, radiation-induced p-CHK1 expression (a marker of SSB DNA repair) was reduced in cells pre-incubated with HER3-ADC. Expression of MRE11, RAD50 and DNA-PK was globally not affected by HER3-ADC and irradiation, except for a slight increase of RAD50. Western blot analysis confirmed the early inhibition by HER3-ADC of AKT, HER3,

and STAT3 phosphorylation (at 60 minutes). The increased expression of cleaved caspase-3 and PARP and reduction of p-BAD at 24h post-treatment (Fig.6B, bottom panel) correlated with the phosphokinome and apoptosome results, but not with the increased number of cleaved caspase-3-positive cells found in tumor xenografts. This discrepancy could be linked to the different treatment doses, time of the analysis after treatment, and cell lines used. Altogether, HER3-ADC inhibited radiation-induced phosphorylation of AKT and STAT pathways, increased expression/activation of pro-apoptotic factors and promoted DNA-damage response in pancreatic cancer cells. These deciding factors partly explained the success of the xenograft experiments, and paved the way for promising clinical study.

Discussion

Increasing the number of patients with PDAC eligible for R0 surgical resection is a major goal for improving the prognosis of pancreatic cancer. Chemoradiation is one way to achieve this aim, but results are quite limited with gemcitabine combination or FOLFIRINOX chemotherapy before chemoradiation [1], mainly due to undesired off-targeted effects. In this study, we demonstrated that the ADC based on MMAE and the anti-HER3 antibody 9F7-F11 is an efficient radiosensitizer to improve chemoradiation in PDAC. Several antibody-based compounds are currently evaluated in the clinic, but none has been approved, alone or combined with radiation, for use in pancreatic cancer. Auristatin-based antibody-drug conjugates, directed against CD70 [25], mesothelin [26], tissue factor [27], nectin-4 [28] and SLC44A4 [29], have been tested as mono or combined therapy [29,30] in patients with PDAC with comparable efficiency as the standard-of-care [30,31]. Although HER3 is expressed in PDAC [8] and regulates survival signaling in tumor cells [9–12], no HER3-specific ADC has been proposed for this indication, particularly in combination with radiation. Radiosensitizing pancreatic tumors with HER3-ADC could have several advantages, such as reducing the doses of both agents to limit adverse side effects, increasing the therapeutic window of radiotherapy, modulating the pancreatic tumor microenvironment, and combining multiple mechanisms of action to reduce the risk of tumor resistance and radioresistance. HER3-ADC fulfills these criteria by inducing arrest in G2/M, the most radiosensitive phase of the cell cycle, promoting caspase 3-mediated signaling and programmed cell death, inhibiting radiation-induced AKT- and STAT-mediated survival, and enhancing DNA DSB formation. Moreover, irradiation favors tumor control by inducing immunogenic modulation, leading to enhanced immune response [32], and also by upregulating tumor cell antigens from the EGFR family that are subject to antibody-dependent cell-mediated cytotoxicity (ADCC) [33]. Therefore, besides radiosensitization, the HER3-ADC+radiation combination could increase ADC-mediated killing by ADCC following radiation-induced cell surface overexpression of tumor antigens (*e.g.,* HER3).

PDAC is characterized by a nearly impenetrable and hypoxic stroma that limits drug delivery to tumor cells, and subsequently treatment effectiveness [34]. This dense desmoplastic stroma consists of vasculature, cellular (immune cells and fibroblasts) and acellular (extracellular matrix containing collagen, fibronectin and hyaluronan) components. Such physical barrier contributes to the failure of targeted monotherapies against antigens expressed on tumor cells (EGFR and HER2) or immune stromal cells (CTLA4 and PD1). Radiation could help to reduce the fibrotic microenvironment by modifying tumor permeability and vasculature, and decreasing interstitial fluid pressure [35], thus favoring the tumor cell uptake of drugs, such as HER3-ADC. Interestingly, it has been suggested that radiation induces a “proteolytic switch” by modulating protease activity in the PDAC microenvironment [4], thus facilitating the localized delivery of therapeutics in tumors. On the other side, HER3-ADC-induced radiosensitization will reduce hypoxia-mediated radioresistance in the PDAC microenvironment.

We also found that HER3-ADC prevents radiation-induced compensatory activation of HER3 and AKT [15,16,36,37]. Moreover, by indirectly affecting HER2/HER3 heterodimer formation upon binding to HER3, as we previously demonstrated for the naked antibody 9F7-F11 [20], HER3-ADC could modulate HER2-mediated activation of ATM/ATR signaling, CHK1 and CHK2 phosphorylation, leading to G2/M arrest [38]. This effect could be additive with the MMAE-mediated upregulation of DNA damage checkpoint proteins in irradiated cells [4]. Incubation with HER3-ADC before irradiation synergistically reduced phosphorylation of STAT3 and STAT5 in pancreatic cancer cells. The STAT family controls cell cycle progression, apoptosis and tumorigenesis, as well as inflammation, through direct phosphorylation of receptor tyrosine kinases (e.g., EGFR) or other kinases (e.g., Src) [39]. In addition, STAT3 plays a prominent role in mediating chemoradiation resistance [40]. Altogether, HER3-ADC-induced radiosensitization of PDAC cells could impair STAT-mediated resistance to chemoradiation, subsequently improving radiation therapy. Following modulation of the DNA repair machinery by HER3-ADC, most unrepaired cells will enter apoptosis after radiation. The ability of HER3-ADC to increase caspase 3 cleavage and PARP activation and to downregulate anti-

apoptotic proteins will promote radiation-induced programmed cell death of pancreatic tumor cells.

In vivo, the MMAE-based HER3-ADC induces a more robust and prolonged radiation response, thus improving tumor control in mice. A single dose of 2.5 to 5 mg/kg HER3-ADC contains 0.04 to 0.08 mg/kg of MMAE, which is less than 10% of the maximum-tolerated dose for this free payload [41]. To date, uncleavable saporin- or MMAF-conjugated HER3-specific ADCs have been pre-clinically proposed as monotherapy for melanoma [42,43]. The anti-HER3 antibody patritumab conjugated to a topoisomerase I inhibitor via a cleavable linker is currently tested in phase I/II trials for patients with metastatic breast cancer [44] and has been pre-clinically demonstrated to be an effective treatment for EGFR-mutant NSCLC with acquired resistance to EGFR TKIs [45]. However, no HER3-specific ADC linked to a cleavable MMAE has been proposed for the radiosensitization of pancreatic tumors. Our MMAE-based HER3-ADC is derived from the 9F7-F11 antibody that has a completely novel pharmacological profile (non-ligand competing allosteric drug) and higher anti-cancer efficacy in the presence of its ligand NRG1 [18]. These 9F7-F11 features perfectly match the clinical profiles of patients with PDAC identified as druggable with anti-HER3 antibodies (*i.e.,* HER3-positive NRG1-addicted or NRG1-rearranged tumors) [46,47]. Moreover, 80% of PDAC mass consists of dense and massive cell stroma with non-tumor cells that secrete growth factors, such as NRG1 [13]. HER3 expression has been correlated with advanced stage of PDAC and decreased survival [8,10]. Together with IGF-1R, HER3 can also serve as drivers of tumor growth and resistance to standard-of-care chemotherapy in metastatic PDAC [12]. In such case of disseminated PDAC where irradiation is not recommended, combining HER3-ADC with chemotherapy could re-sensitize pancreatic cancer cells to chemotherapy, similarly as those observed with patritumab-ADC in TKI-resistant NSCLC [45].

Next-generation payloads, with optimized linkers, spacers, and well-defined drug-antibody ratios [48], could be investigated to further improve the radiosensitizing effect we observed. In pancreatic cancer, HER3-ADC could also be coupled with magnetic resonance imaging-guided radiotherapy, a new technique that improves soft tissue contrast and target

identification together with accurate dose calculation and collimated X-ray beam delivery [49,50]. In such way, the HER3-ADC plus irradiation combination would plausibly help to increase the rate of R0 resection for patients with borderline resectable pancreatic cancer.

Acknowledgements

We thank S. Bousquié (IRCM) for cell culture and antibody production. The staff at the IRCM animal facility, the PDX and MRI platforms, and the RHEM histology facility are greatly acknowledged. We also thank the ICM Radiotherapy Department for their help with irradiation. J-F. Prost, J-M. Barret and O. Dubreuil (GamaMabs Pharma) are also acknowledged for fruitful discussion and advice.

References

1. Ducreux M, Cuhna AS, Caramella C, Hollebecque A, Burtin P, Goéré D, Seufferlein T, Haustermans K, Van Laethem JL, Conroy T, Arnold D, ESMO Guidelines Committee. Cancer of the pancreas: ESMO Clinical Practice Guidelines for diagnosis, treatment and follow-up. *Ann Oncol* 2015;26 Suppl 5:v56-68.

2. Rahib L, Smith BD, Aizenberg R, Rosenzweig AB, Fleshman JM, Matrisian LM. Projecting cancer incidence and deaths to 2030: the unexpected burden of thyroid, liver, and pancreas cancers in the United States. *Cancer Res* 2014;74:2913–21.

3. Seshacharyulu P, Baine MJ, Souchek JJ, Menning M, Kaur S, Yan Y, Ouellette MM, Jain M, Lin C, Batra SK. Biological determinants of radioresistance and their remediation in pancreatic cancer. *Biochim Biophys Acta* 2017;1868:69–92.

4. Buckel L, Savariar EN, Crisp JL, Jones KA, Hicks AM, Scanderbeg DJ, Nguyen QT, Sicklick JK, Lowy AM, Tsien RY, Advani SJ. Tumor radiosensitization by monomethyl auristatin E: mechanism of action and targeted delivery. *Cancer Res* 2015;75:1376–87.

5. Adams SR, Yang HC, Savariar EN, Aguilera J, Crisp JL, Jones KA, Whitney MA, Lippman SM, Cohen EEW, Tsien RY, Advani SJ. Anti-tubulin drugs conjugated to anti-ErbB antibodies selectively radiosensitize. *Nat Commun* 2016;7:13019.

6. Safran H, Iannitti D, Ramanathan R, Schwartz JD, Steinhoff M, Nauman C, Hesketh P, Rathore R, Wolff R, Tantravahi U, Hughes TM, Maia C, et al. Herceptin and gemcitabine for metastatic pancreatic cancers that overexpress HER-2/neu. *Cancer Invest* 2004;22:706–12.

7. Philip PA, Benedetti J, Corless CL, Wong R, O'Reilly EM, Flynn PJ, Rowland KM, Atkins JN, Mirtsching BC, Rivkin SE, Khorana AA, Goldman B, et al. Phase III study comparing gemcitabine plus cetuximab versus gemcitabine in patients with advanced pancreatic adenocarcinoma: Southwest Oncology Group-directed intergroup trial S0205. *J Clin Oncol* 2010;28:3605–10.

8. Friess H, Yamanaka Y, Kobrin MS, Do DA, Büchler MW, Korc M. Enhanced erbB-3 expression in human pancreatic cancer correlates with tumor progression. *Clin Cancer Res* 1995;1:1413–20.

9. Arnoletti JP, Buchsbaum DJ, Huang Z, Hawkins AE, Khazaeli MB, Kraus MH, Vickers SM. Mechanisms of resistance to Erbitux (anti-epidermal growth factor receptor) combination therapy in pancreatic adenocarcinoma cells. *J Gastrointest Surg* 2004;8:960–9; discussion 969-970.

10. Liles JS, Arnoletti JP, Tzeng C-WD, Howard JH, Kossenkov AV, Kulesza P, Heslin MJ, Frolov A. ErbB3 expression promotes tumorigenesis in pancreatic adenocarcinoma. *Cancer Biol Ther* 2010;10:555–63.

11. Fitzgerald JB, Johnson BW, Baum J, Adams S, Iadevaia S, Tang J, Rimkunas V, Xu L, Kohli N, Rennard R, Razlog M, Jiao Y, et al. MM-141, an IGF-IR- and ErbB3-directed bispecific antibody, overcomes network adaptations that limit activity of IGF-IR inhibitors. *Mol Cancer Ther* 2014;13:410–25.

12. Camblin AJ, Pace EA, Adams S, Curley MD, Rimkunas V, Nie L, Tan G, Bloom T, Iadevaia S, Baum J, Minx C, Czibere A, et al. Dual Inhibition of IGF-1R and ErbB3

Enhances the Activity of Gemcitabine and Nab-Paclitaxel in Preclinical Models of Pancreatic Cancer. *Clin Cancer Res* 2018;

13. Liles JS, Arnoletti JP, Kossenkov AV, Mikhaylina A, Frost AR, Kulesza P, Heslin MJ, Frolov A. Targeting ErbB3-mediated stromal-epithelial interactions in pancreatic ductal adenocarcinoma. *Br J Cancer* 2011;105:523–33.

14. Contessa JN, Abell A, Mikkelsen RB, Valerie K, Schmidt-Ullrich RK. Compensatory ErbB3/c-Src signaling enhances carcinoma cell survival to ionizing radiation. *Breast Cancer Res Treat* 2006;95:17–27.

15. Li C, Brand TM, Iida M, Huang S, Armstrong EA, van der Kogel A, Wheeler DL. Human epidermal growth factor receptor 3 (HER3) blockade with U3-1287/AMG888 enhances the efficacy of radiation therapy in lung and head and neck carcinoma. *Discov Med* 2013;16:79–92.

16. Li C, Huang S, Armstrong EA, Francis DM, Werner LR, Sliwkowski MX, van der Kogel A, Harari PM. Antitumor Effects of MEHD7945A, a Dual-Specific Antibody against EGFR and HER3, in Combination with Radiation in Lung and Head and Neck Cancers. *Mol Cancer Ther* 2015;14:2049–59.

17. Dote H, Cerna D, Burgan WE, Camphausen K, Tofilon PJ. ErbB3 expression predicts tumor cell radiosensitization induced by Hsp90 inhibition. *Cancer Res* 2005;65:6967–75.

18. Le Clorennec C, Bazin H, Dubreuil O, Larbouret C, Ogier C, Lazrek Y, Garambois V, Poul M-A, Mondon P, Barret J-M, Mathis G, Prost J-F, et al. Neuregulin 1 Allosterically Enhances the Antitumor Effects of the Noncompeting Anti-HER3 Antibody 9F7-F11 by Increasing Its Binding to HER3. *Mol Cancer Ther* 2017;16:1312–23.

19. Lazrek Y, Dubreuil O, Garambois V, Gaborit N, Larbouret C, Le Clorennec C, Thomas G, Leconet W, Jarlier M, Pugnière M, Vié N, Robert B, et al. Anti-HER3 domain 1 and 3 antibodies reduce tumor growth by hindering HER2/HER3 dimerization and AKT-induced MDM2, XIAP, and FoxO1 phosphorylation. *Neoplasia* 2013;15:335–47.

20. Thomas G, Chardès T, Gaborit N, Mollevi C, Leconet W, Robert B, Radosevic-Robin N, Penault-Llorca F, Gongora C, Colombo P-E, Lazrek Y, Bras-Goncalves R, et al. HER3 as biomarker and therapeutic target in pancreatic cancer: new insights in pertuzumab therapy in preclinical models. *Oncotarget* 2014;5:7138–48.

21. Le Clorennec C, Lazrek Y, Dubreuil O, Larbouret C, Poul M-A, Mondon P, Melino G, Pèlegrin A, Chardès T. The anti-HER3 (ErbB3) therapeutic antibody 9F7-F11 induces HER3 ubiquitination and degradation in tumors through JNK1/2- dependent ITCH/AIP4 activation. *Oncotarget* 2016;

22. Terasima T, Tolmach LJ. Variations in several responses of HeLa cells to x-irradiation during the division cycle. *Biophys J* 1963;3:11–33.

23. Doronina SO, Toki BE, Torgov MY, Mendelsohn BA, Cerveny CG, Chace DF, DeBlanc RL, Gearing RP, Bovee TD, Siegall CB, Francisco JA, Wahl AF, et al. Development of potent monoclonal antibody auristatin conjugates for cancer therapy. *Nat Biotechnol* 2003;21:778–84.

24. Leconet W, Larbouret C, Chardès T, Thomas G, Neiveyans M, Busson M, Jarlier M, Radosevic-Robin N, Pugnière M, Bernex F, Penault-Llorca F, Pasquet J-M, et al.

Preclinical validation of AXL receptor as a target for antibody-based pancreatic cancer immunotherapy. *Oncogene* 2014;33:5405–14.

25. Ryan MC, Kostner H, Gordon KA, Duniho S, Sutherland MK, Yu C, Kim KM, Nesterova A, Anderson M, McEarchern JA, Law C-L, Smith LM. Targeting pancreatic and ovarian carcinomas using the auristatin-based anti-CD70 antibody-drug conjugate SGN-75. *Br J Cancer* 2010;103:676–84.

26. Scales SJ, Gupta N, Pacheco G, Firestein R, French DM, Koeppen H, Rangell L, Barry-Hamilton V, Luis E, Chuh J, Zhang Y, Ingle GS, et al. An antimesothelin-monomethyl auristatin e conjugate with potent antitumor activity in ovarian, pancreatic, and mesothelioma models. *Mol Cancer Ther* 2014;13:2630–40.

27. Koga Y, Manabe S, Aihara Y, Sato R, Tsumura R, Iwafuji H, Furuya F, Fuchigami H, Fujiwara Y, Hisada Y, Yamamoto Y, Yasunaga M, et al. Antitumor effect of antitissue factor antibody-MMAE conjugate in human pancreatic tumor xenografts. *Int J Cancer* 2015;137:1457–66.

28. Challita-Eid PM, Satpayev D, Yang P, An Z, Morrison K, Shostak Y, Raitano A, Nadell R, Liu W, Lortie DR, Capo L, Verlinsky A, et al. Enfortumab Vedotin Antibody-Drug Conjugate Targeting Nectin-4 Is a Highly Potent Therapeutic Agent in Multiple Preclinical Cancer Models. *Cancer Res* 2016;76:3003–13.

29. Mattie M, Raitano A, Morrison K, Morrison K, An Z, Capo L, Verlinsky A, Leavitt M, Ou J, Nadell R, Aviña H, Guevara C, et al. The Discovery and Preclinical Development of ASG-5ME, an Antibody-Drug Conjugate Targeting SLC44A4-Positive Epithelial Tumors Including Pancreatic and Prostate Cancer. *Mol Cancer Ther* 2016;15:2679–87.

30. Yao H-P, Feng L, Zhou J-W, Zhang R-W, Wang M-H. Therapeutic evaluation of monoclonal antibody-maytansinoid conjugate as a model of RON-targeted drug delivery for pancreatic cancer treatment. *Am J Cancer Res* 2016;6:937–56.

31. Strop P, Tran T-T, Dorywalska M, Delaria K, Dushin R, Wong OK, Ho W-H, Zhou D, Wu A, Kraynov E, Aschenbrenner L, Han B, et al. RN927C, a Site-Specific Trop-2 Antibody-Drug Conjugate (ADC) with Enhanced Stability, Is Highly Efficacious in Preclinical Solid Tumor Models. *Mol Cancer Ther* 2016;15:2698–708.

32. Kumari A, Simon SS, Moody TD, Garnett-Benson C. Immunomodulatory effects of radiation: what is next for cancer therapy? *Future Oncol* 2016;12:239–56.

33. Wattenberg MM, Kwilas AR, Gameiro SR, Dicker AP, Hodge JW. Expanding the use of monoclonal antibody therapy of cancer by using ionising radiation to upregulate antibody targets. *Br J Cancer* 2014;110:1472–80.

34. Adiseshaiah PP, Crist RM, Hook SS, McNeil SE. Nanomedicine strategies to overcome the pathophysiological barriers of pancreatic cancer. *Nat Rev Clin Oncol* 2016;13:750–65.

35. Znati CA, Rosenstein M, Boucher Y, Epperly MW, Bloomer WD, Jain RK. Effect of radiation on interstitial fluid pressure and oxygenation in a human tumor xenograft. *Cancer Res* 1996;56:964–8.

36. Huang S, Li C, Armstrong EA, Peet CR, Saker J, Amler LC, Sliwkowski MX, Harari PM. Dual targeting of EGFR and HER3 with MEHD7945A overcomes acquired resistance to EGFR inhibitors and radiation. *Cancer Res* 2013;73:824–33.

37. Francis DM, Huang S, Armstrong EA, Werner LR, Hullett C, Li C, Morris ZS, Swick AD, Kragh M, Lantto J, Kimple RJ, Harari PM. Pan-HER Inhibitor Augments Radiation Response in Human Lung and Head and Neck Cancer Models. *Clin Cancer Res* 2016;22:633–43.

38. Yan Y, Hein AL, Greer PM, Wang Z, Kolb RH, Batra SK, Cowan KH. A novel function of HER2/Neu in the activation of G2/M checkpoint in response to γ-irradiation. *Oncogene* 2015;34:2215–26.

39. Silva CM. Role of STATs as downstream signal transducers in Src family kinase-mediated tumorigenesis. *Oncogene* 2004;23:8017–23.

40. Spitzner M, Ebner R, Wolff HA, Ghadimi BM, Wienands J, Grade M. STAT3: A Novel Molecular Mediator of Resistance to Chemoradiotherapy. *Cancers (Basel)* 2014;6:1986–2011.

41. Francisco JA, Cerveny CG, Meyer DL, Mixan BJ, Klussman K, Chace DF, Rejniak SX, Gordon KA, DeBlanc R, Toki BE, Law C-L, Doronina SO, et al. cAC10-vcMMAE, an anti-CD30-monomethyl auristatin E conjugate with potent and selective antitumor activity. *Blood* 2003;102:1458–65.

42. Capone E, Giansanti F, Ponziani S, Lamolinara A, Iezzi M, Cimini A, Angelucci F, Sorda RL, Laurenzi VD, Natali PG, Ippoliti R, Iacobelli S, et al. EV20-Sap, a novel anti-HER-3 antibody-drug conjugate, displays promising antitumor activity in melanoma. *Oncotarget* 2017;8:95412–24.

43. Capone E, Lamolinara A, D'Agostino D, Rossi C, De Laurenzi V, Iezzi M, Iacobelli S, Sala G. EV20-mediated delivery of cytotoxic auristatin MMAF exhibits potent therapeutic efficacy in cutaneous melanoma. *J Control Release* 2018;277:48–56.

44. Kogawa T, Yonemori K, Naito Y, Noguchi E, Shimizu C, Tamura K, Hosono A, Matsubara N, Sugihara M, Ogawa H, Majima S, Yu C, et al. Phase 1/2, multicenter, non-randomized, open-label, multiple-dose first-in-class study of U3-1402 (anti-HER3 antibody-drug conjugate) in subjects with HER3-positive metastatic breast cancer. *J Clin Oncol* 2017;35:60s.

45. Yonesaka K, Takegawa N, Watanabe S, Haratani K, Kawakami H, Sakai K, Chiba Y, Maeda N, Kagari T, Hirotani K, Nishio K, Nakagawa K. An HER3-targeting antibody–drug conjugate incorporating a DNA topoisomerase I inhibitor U3-1402 conquers EGFR tyrosine kinase inhibitor-resistant NSCLC. *Oncogene [Internet]* 2018;Available from: https://doi.org/10.1038/s41388-018-0517-4

46. Drilon A, Somwar R, Mangatt BP, Edgren H, Desmeules P, Ruusulehto A, Smith RS, Delasos L, Vojnic M, Plodkowski AJ, Sabari J, Ng K, et al. Response to ERBB3-Directed Targeted Therapy in NRG1-Rearranged Cancers. *Cancer Discov* 2018;8:686–95.

47. Yonesaka K, Hirotani K, von Pawel J, Dediu M, Chen S, Copigneaux C, Nakagawa K. Circulating heregulin level is associated with the efficacy of patritumab combined with erlotinib in patients with non-small cell lung cancer. *Lung Cancer* 2017;105:1–6.

48. Beck A, Goetsch L, Dumontet C, Corvaïa N. Strategies and challenges for the next generation of antibody-drug conjugates. *Nat Rev Drug Discov* 2017;16:315–37.

49. Kersemans V, Beech JS, Gilchrist S, Kinchesh P, Allen PD, Thompson J, Gomes AL, D'Costa Z, Bird L, Tullis IDC, Newman RG, Corroyer-Dulmont A, et al. An efficient and robust MRI-guided radiotherapy planning approach for targeting abdominal organs and tumours in the mouse. *PLoS ONE* 2017;12:e0176693.

50. Schneider S, Jølck RI, Troost EGC, Hoffmann AL. Quantification of MRI visibility and artifacts at 3T of liquid fiducial marker in a pancreas tissue-mimicking phantom. *Med Phys* 2018;45:37–47.

Figure legends

Figure 1. Characterization of the MMAE-based HER3-ADC. (**A**) ELISA binding curves of HER3-ADC, 9F7-F11 and negative control antibody using HER3 ECD as capture antigen. The EC_{50} were calculated using GraphPad Prism 6. (**B**) Time-dependent internalization of fluorescein-labeled HER3-ADC in MCF7 cells at 4°C and 37°C. (**C**) Dose-dependent effect of HER3-ADC, 9F7-F11 and control antibody on viability of the pancreatic cancer cell lines BxPC3 and HPAC, and the PDX-derived cell line P4604, with or without stimulation by NRG1. M, medium alone. (**D**) Clonogenic survival (Giemsa staining) of BxPC3 and HPAC cells (in 10% FCS) at day 12 after incubation with different concentrations of HER3-ADC.

Figure 2. HER3-ADC blocks cells in the G2/M phase and favors apoptosis of pancreatic cancer cells. (**A**) Time-dependent accumulation of BxPC3 in the G2/M phase after incubation with HER3-ADC, 9F7-F11, or medium alone. (**B**) Cell cycle profile of BxPC3 cells incubated with HER3-ADC (different concentrations), 9F7-F11, or medium alone for 24h, stained with PI and analyzed by flow cytometry. (**C**) Percentage of BxPC3 cells in the sub-G1 phase after incubation with HER3-ADC (different concentrations), 9F7-F11, or medium alone. (**D**) Percentage of early-apoptotic (annexin V-positive and 7-AAD-negative), and late-apoptotic (double-positive) BxPC3 cells after incubation with HER3-ADC (different concentrations), 9F7-F11, or medium alone. All experiments have been performed in triplicates

Figure 3. HER3-ADC radiosensitizes pancreatic cancer cells. (**A**) Clonogenic survival (Giemsa staining) of BxPC3, HPAC, and P4604 cells at day 14 after exposure to 2 or 5μg/ml HER3-ADC and/or irradiation (2Gy). (**B**) Measurement of absorbance at 595nm of ethanol-solubilized colonies at day 14. 100% value was calculated from absorbance measured in medium-treated cells.

Figure 4. HER3-ADC increases the radiation response in mice. Nude mice were xenografted with BxPC3 (**A**), HPAC (**B**) and PDX P4604 cells (**C**). Mice harboring BxPC3 and HPAC cell xenografts were treated with HER3-ADC (full gray solid line) or irradiation (dark hatched line) alone, or HER3-ADC 24h before irradiation (gray hatched line), twice a week for 4 weeks. The control group received saline (full black solid line). Mice harboring PDX P4604 received one single intravenous injection of HER3-ADC and/or one single radiation fraction (24h after HER3-ADC). Kaplan-Meier survival curves were calculated when tumors reached a volume of 1000 mm^3 and mice were sacrificed. (**D**) Immunohistochemistry analysis of KI67 (proliferation marker) and cleaved caspase-3 expression in PDX P4604 xenografts at day 15 of treatment. Data were quantified with Image Scope. (**E and F**). Immunohistochemistry analysis (**G**) and quantification (**H**) of NRG1 and HER3 expression in surgical tumor biopsies from 45 patients with PDAC.

Figure 5. HER3-ADC increases DNA double-strand break formation in irradiated pancreatic cancer cells. Radiation-induced DNA damage throughout the cell cycle was measured using an anti-γH2AX antibody and PI staining. (**A**) Flow cytometry profiles of γH2AX levels and DNA content of BxPC3 cells that received 1μg/ml HER3-ADC and/or 2Gy irradiation. (**B**) Quantification of γH2AX-positive BxPC3 cells. **(C)** Representative images of nuclear γH2AX foci in BxPC3 cells incubated with 5μg/ml HER3-ADC or 9F7-F11, combined or not with irradiation (2Gy). (**D**) Mean number of γH2AX foci per nucleus. (**E**) Quantification of nuclei with up to 15 γH2AX foci.

Figure 6. HER3-ADC inhibits radiation-induced survival pathways, and favors apoptotic signaling. (A) Human stress and apoptosis, phospho-kinase and phospho-STAT array profiling in BxPC3 cells exposed to HER3-ADC (1μg/ml), irradiation (2Gy) (IR), or both (irradiation 24h after HER3-ADC). Spot intensities were quantified by densitometry with Image J, and normalized to tubulin expression. Heatmaps indicate the expression changes

for each protein. Down- (blue) or up-regulation (red) was calculated relative to the 100% normal expression in control cells (medium alone; white). **(B)** Western blot analysis of proteins involved in the DNA damage repair, survival and apoptosis pathways. BxPC3 cells were incubated with 1μg/ml HER3-ADC 24h before irradiation (2Gy) (IR). Cells were harvested and lysed 1h and 24h post-irradiation. After electrophoresis, proteins were detected using the appropriate antibodies. M: BxPC3 cells stimulated only with NRG1.

Figure 1

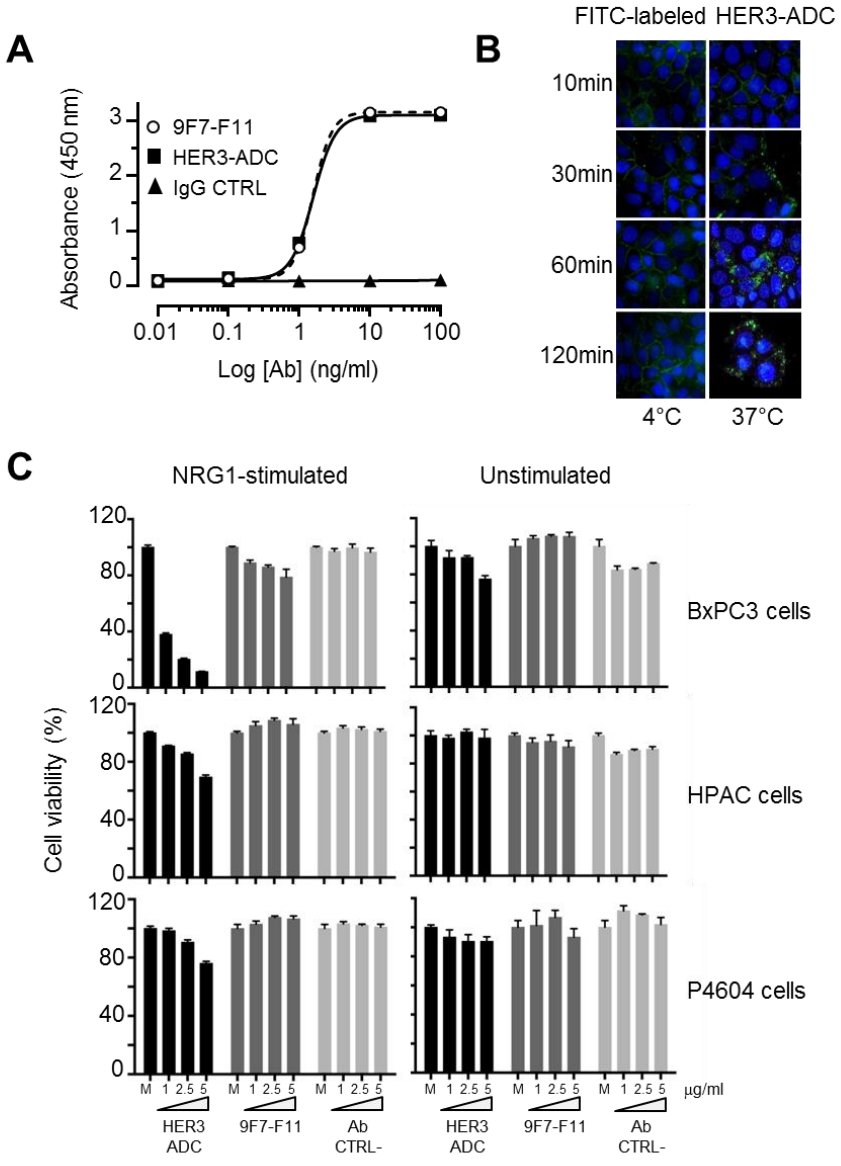
A
Absorbance (450 nm)
9F7-F11
HER3-ADC
IgG CTRL
Log [Ab] (ng/ml)
B
FITC-labeled HER3-ADC
10min
30min
60min
120min
4°C
37°C
C
NRG1-stimulated
Unstimulated
Cell viability (%)
BxPC3 cells
HPAC cells
P4604 cells
M 1 2.5 5
µg/ml
HER3 ADC
9F7-F11
Ab CTRL-
D
HER3-ADC (µg/ml)
M
1
2.5
5
12 days-clonogenic survival of BxPC3 cancer cells
12 days-clonogenic survival of HPAC cancer cells

Figure 2

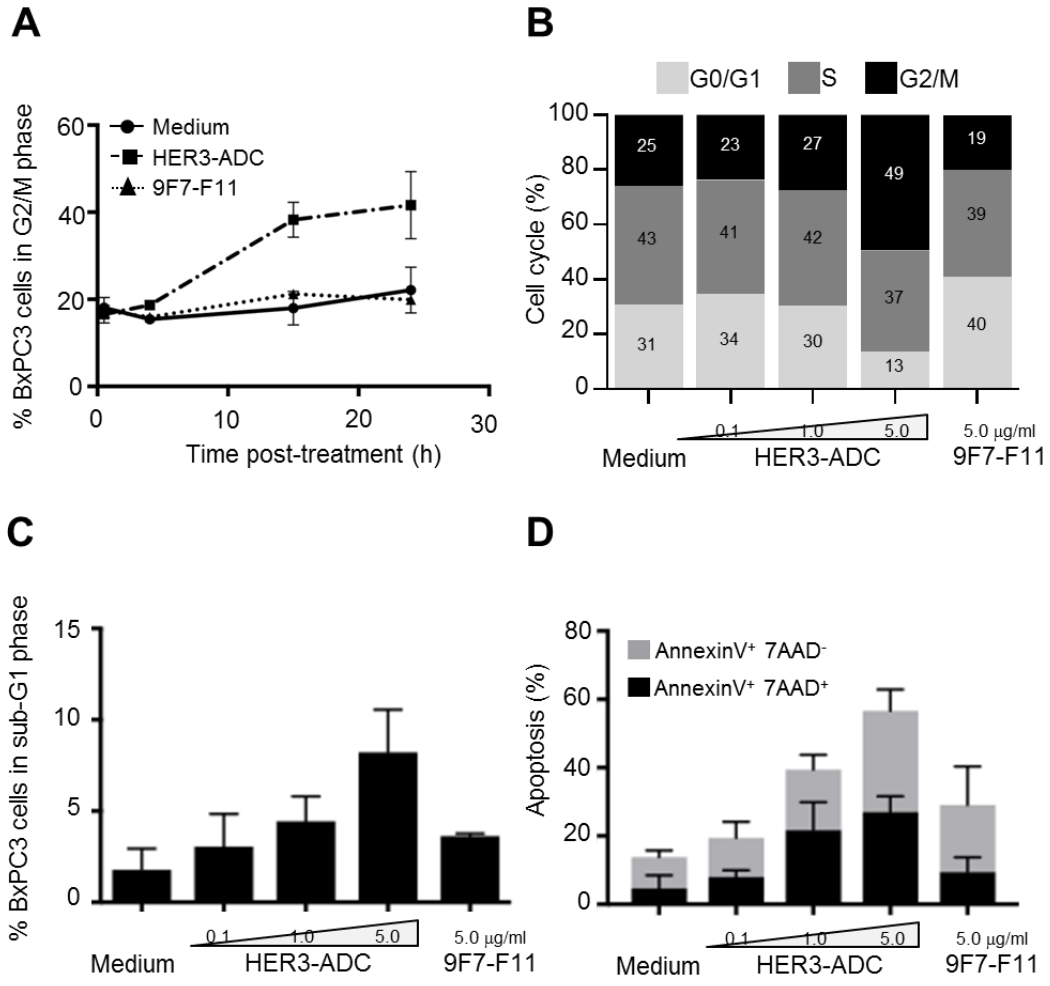
A
% BxPC3 cells in G2/M phase
Medium
HER3-ADC
9F7-F11
Time post-treatment (h)
B
G0/G1
S
G2/M
Cell cycle (%)
25
43
31
23
41
34
27
42
30
49
37
13
19
39
40
Medium
HER3-ADC
0.1
1.0
5.0
5.0 µg/ml
9F7-F11
C
% BxPC3 cells in sub-G1 phase
Medium
HER3-ADC
9F7-F11
D
AnnexinV+ 7AAD-
AnnexinV+ 7AAD+
Apoptosis (%)
Medium
HER3-ADC
9F7-F11

Figure 3

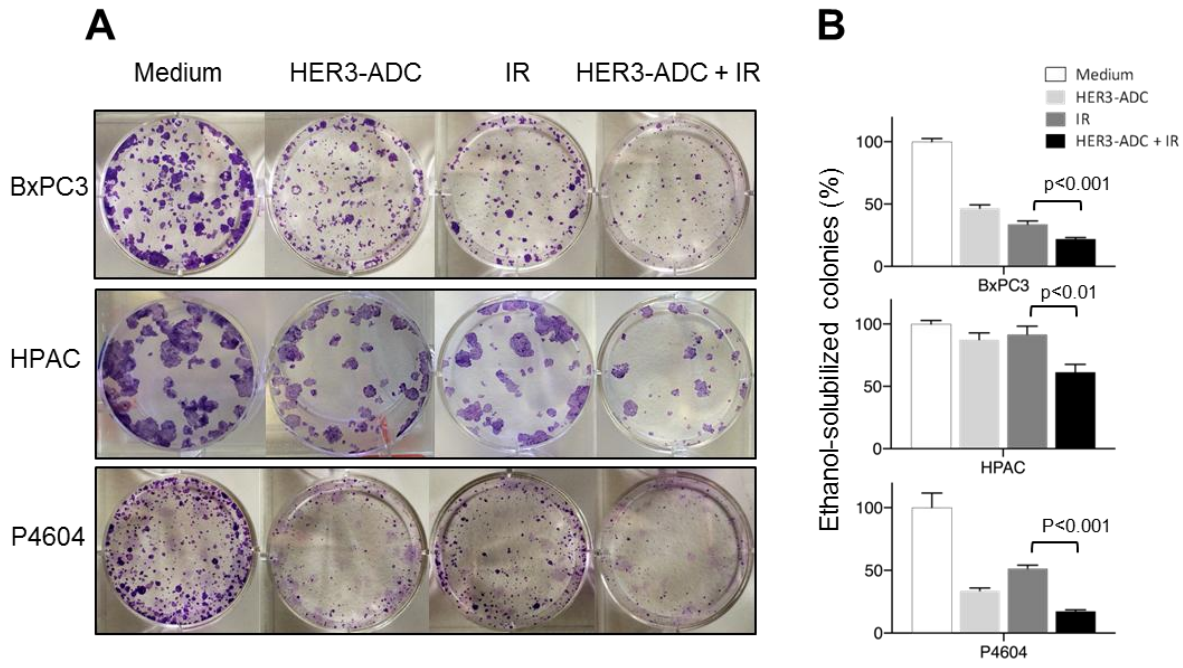
A
Medium
HER3-ADC
IR
HER3-ADC + IR
BxPC3
HPAC
P4604
B
Medium
HER3-ADC
IR
HER3-ADC + IR
Ethanol-solubilized colonies (%)
100
50
0
p<0.001
BxPC3
p<0.01
HPAC
P<0.001
P4604

Figure 4

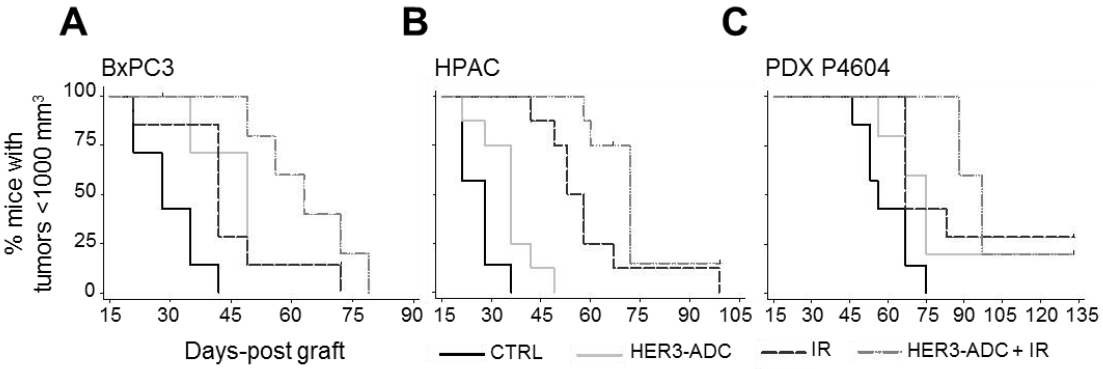

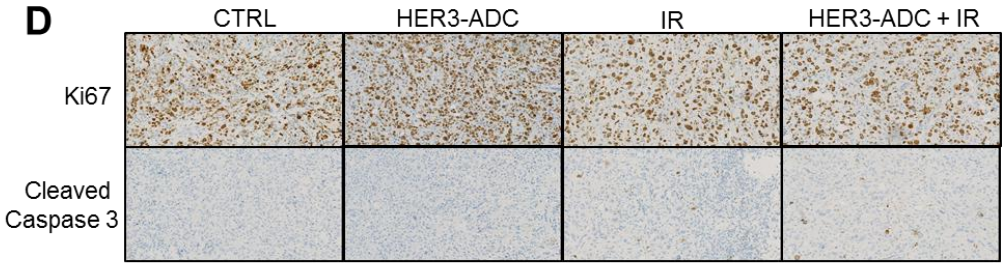

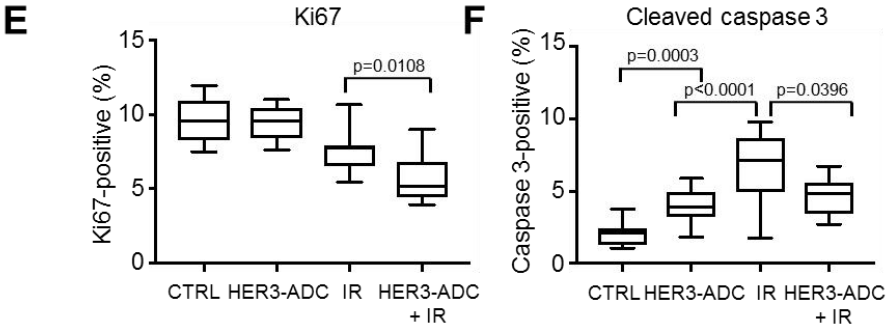

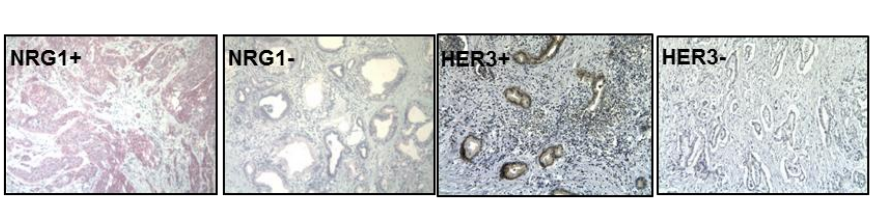

H

NRG1 and HER3 expression in PDAC samples			
	NRG1	HER3	NRG1+HER3
Number	21/45	10/45	7/45
%	46	22	15

Figure 5

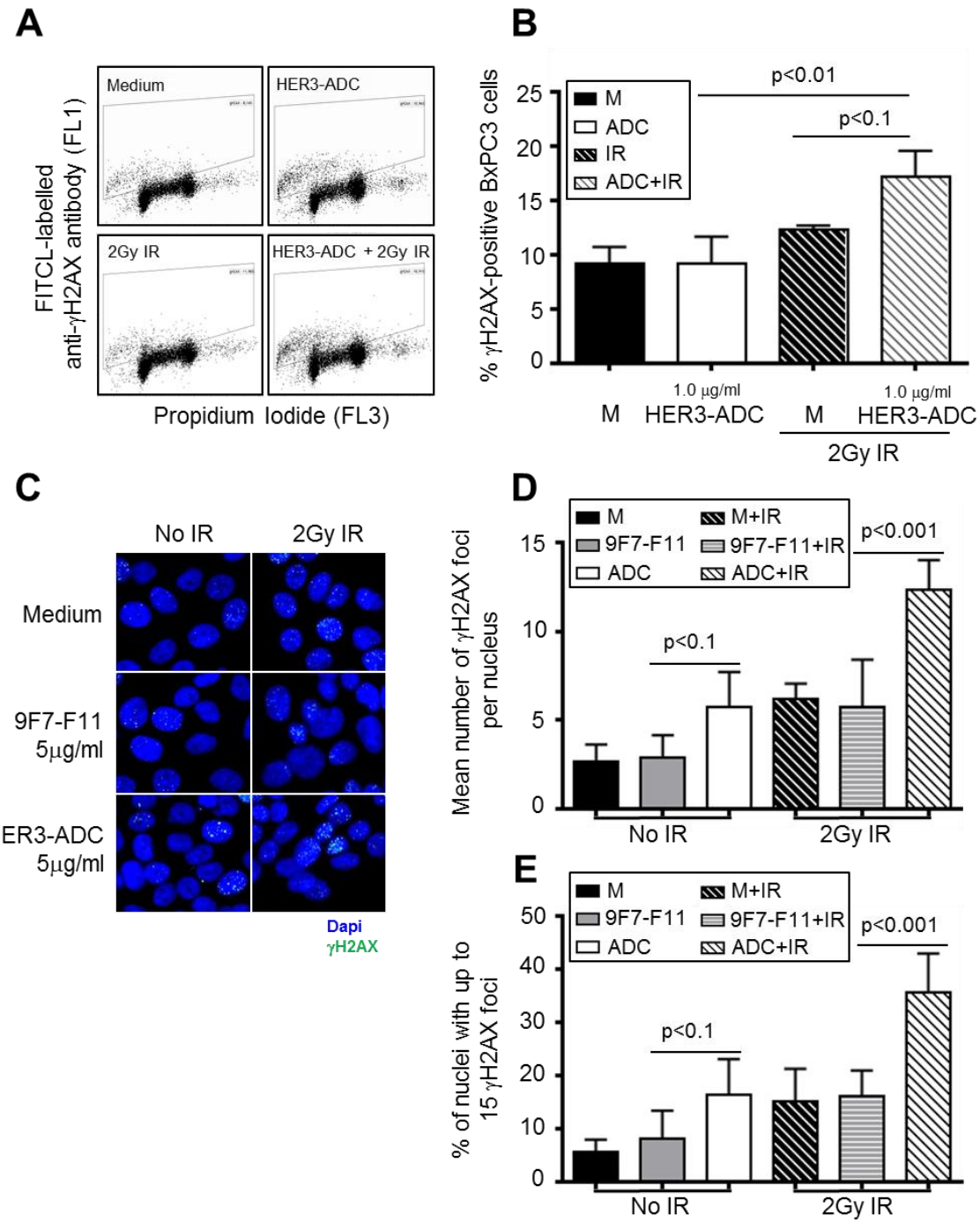
A
Medium
HER3-ADC
2Gy IR
HER3-ADC + 2Gy IR
FITCL-labelled anti-γH2AX antibody (FL1)
Propidium Iodide (FL3)
B
% γH2AX-positive BxPC3 cells
M
ADC
IR
ADC+IR
p<0.01
p<0.1
1.0 μg/ml
M
HER3-ADC
M
HER3-ADC
2Gy IR
C
No IR
2Gy IR
Medium
9F7-F11 5μg/ml
HER3-ADC 5μg/ml
Dapi
γH2AX
D
Mean number of γH2AX foci per nucleus
M
M+IR
9F7-F11
9F7-F11+IR
ADC
ADC+IR
p<0.001
p<0.1
No IR
2Gy IR
E
% of nuclei with up to 15 γH2AX foci
M
M+IR
9F7-F11
9F7-F11+IR
ADC
ADC+IR
p<0.001
p<0.1
No IR
2Gy IR

Figure 6

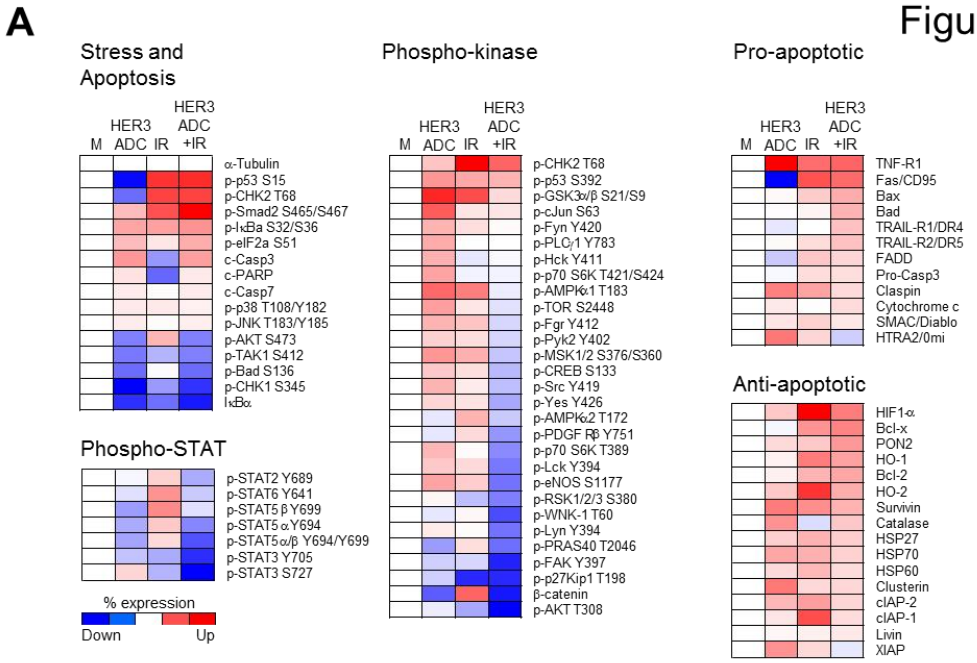
A
Stress and Apoptosis
M
HER3 ADC
IR
HER3 ADC +IR
α-Tubulin
p-p53 S15
p-CHK2 T68
p-Smad2 S465/S467
p-IκBa S32/S36
p-eIF2a S51
c-Casp3
c-PARP
c-Casp7
p-p38 T108/Y182
p-JNK T183/Y185
p-AKT S473
p-TAK1 S412
p-Bad S136
p-CHK1 S345
IκBα
Phospho-STAT
p-STAT2 Y689
p-STAT6 Y641
p-STAT5 β Y699
p-STAT5 α Y694
p-STAT5 α/β Y694/Y699
p-STAT3 Y705
p-STAT3 S727
% expression
Down
Up
Phospho-kinase
p-CHK2 T68
p-p53 S392
p-GSK3α/β S21/S9
p-cJun S63
p-Fyn Y420
p-PLCγ1 Y783
p-Hck Y411
p-p70 S6K T421/S424
p-AMPKα1 T183
p-TOR S2448
p-Fgr Y412
p-Pyk2 Y402
p-MSK1/2 S376/S360
p-CREB S133
p-Src Y419
p-Yes Y426
p-AMPKα2 T172
p-PDGF Rβ Y751
p-p70 S6K T389
p-Lck Y394
p-eNOS S1177
p-RSK1/2/3 S380
p-WNK-1 T60
p-Lyn Y394
p-PRAS40 T2046
p-FAK Y397
p-p27Kip1 T198
β-catenin
p-AKT T308
Pro-apoptotic
TNF-R1
Fas/CD95
Bax
Bad
TRAIL-R1/DR4
TRAIL-R2/DR5
FADD
Pro-Casp3
Claspin
Cytochrome c
SMAC/Diablo
HTRA2/0mi
Anti-apoptotic
HIF1-α
Bcl-x
PON2
HO-1
Bcl-2
HO-2
Survivin
Catalase
HSP27
HSP70
HSP60
Clusterin
cIAP-2
cIAP-1
Livin
XIAP

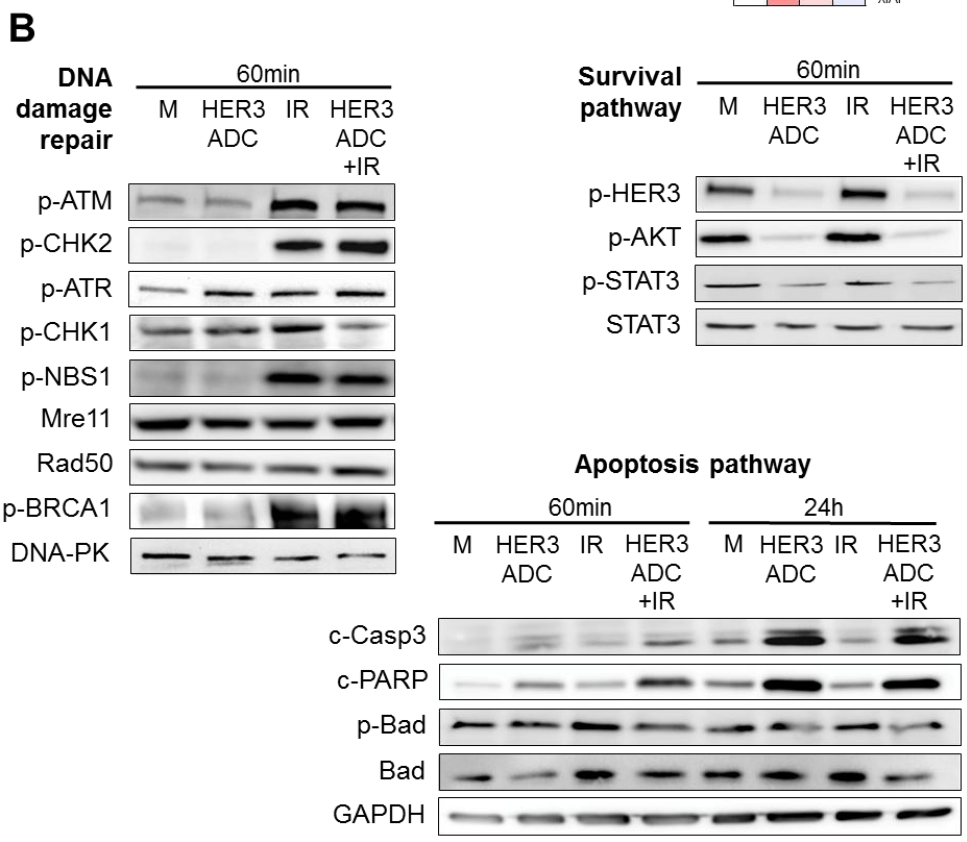
B
DNA damage repair
60min
M
HER3 ADC
IR
HER3 ADC +IR
p-ATM
p-CHK2
p-ATR
p-CHK1
p-NBS1
Mre11
Rad50
p-BRCA1
DNA-PK
Survival pathway
p-HER3
p-AKT
p-STAT3
STAT3
Apoptosis pathway
60min
24h
c-Casp3
c-PARP
p-Bad
Bad
GAPDH

Figure S1

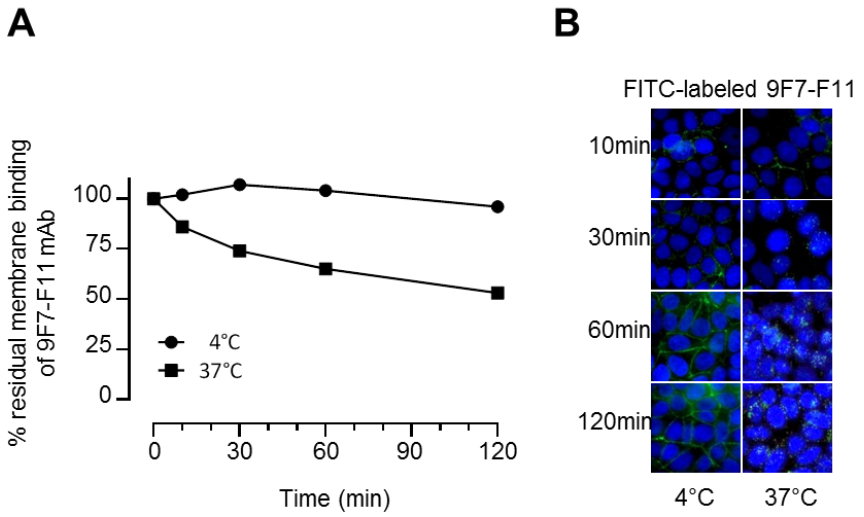

Supplementary Figure S1. The naked anti-HER3 antibody 9F7-F11 is internalized in tumor cells. (A) A549 cells were pre-incubated with 9F7-F11 for 1h at 4°C for pre-binding, before incubation at 4°C or 37°C for 10, 30, 60 or 120 min. Cells were then fixed in 3% PFA, washed and incubated with a FITC-conjugated secondary antibody at 4°C for 45min to assess the residual membrane binding by flow cytometry. **(B)** Immunofluorescence images of time-dependent internalization of fluorescein-labeled 9F7-F11 in MCF7 cells at 4°C and 37°C. MAb, monoclonal antibody.

Figure S2

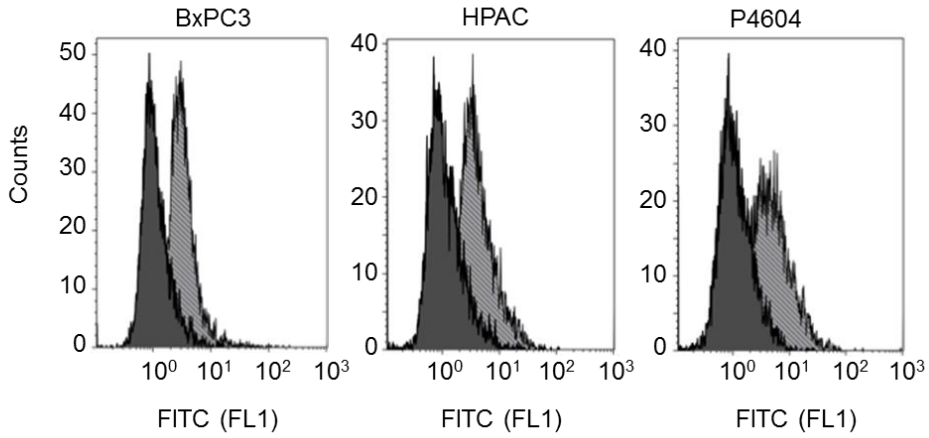

Supplementary Figure S2. HER3 expression in the pancreatic cancer cell lines BxPC3 and HPAC, and the PDX-derived cell line P4604 was determined by flow cytometry.

Figure S3

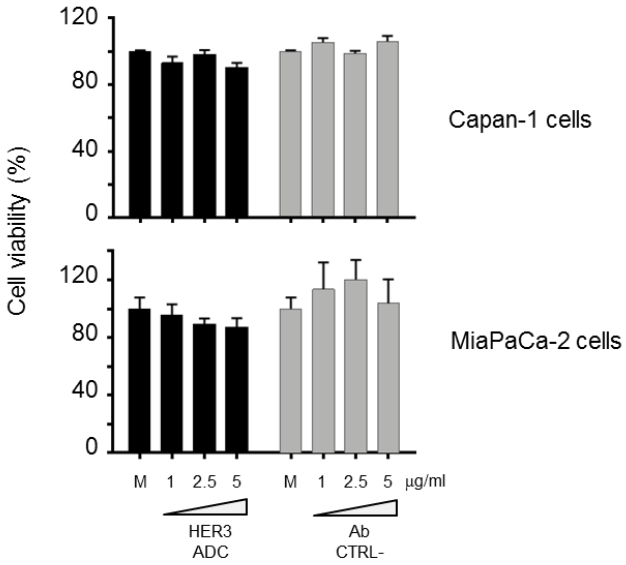

Supplementary Figure S3. HER3-ADC did not affect cell viability of HER3-negative cells. Dose-dependent effect of HER3-ADC and control antibody on viability of the HER3-negative pancreatic cancer cell lines Capan-1 and MiaPaca-2, without stimulation by NRG1. M, medium alone.

Figure S4

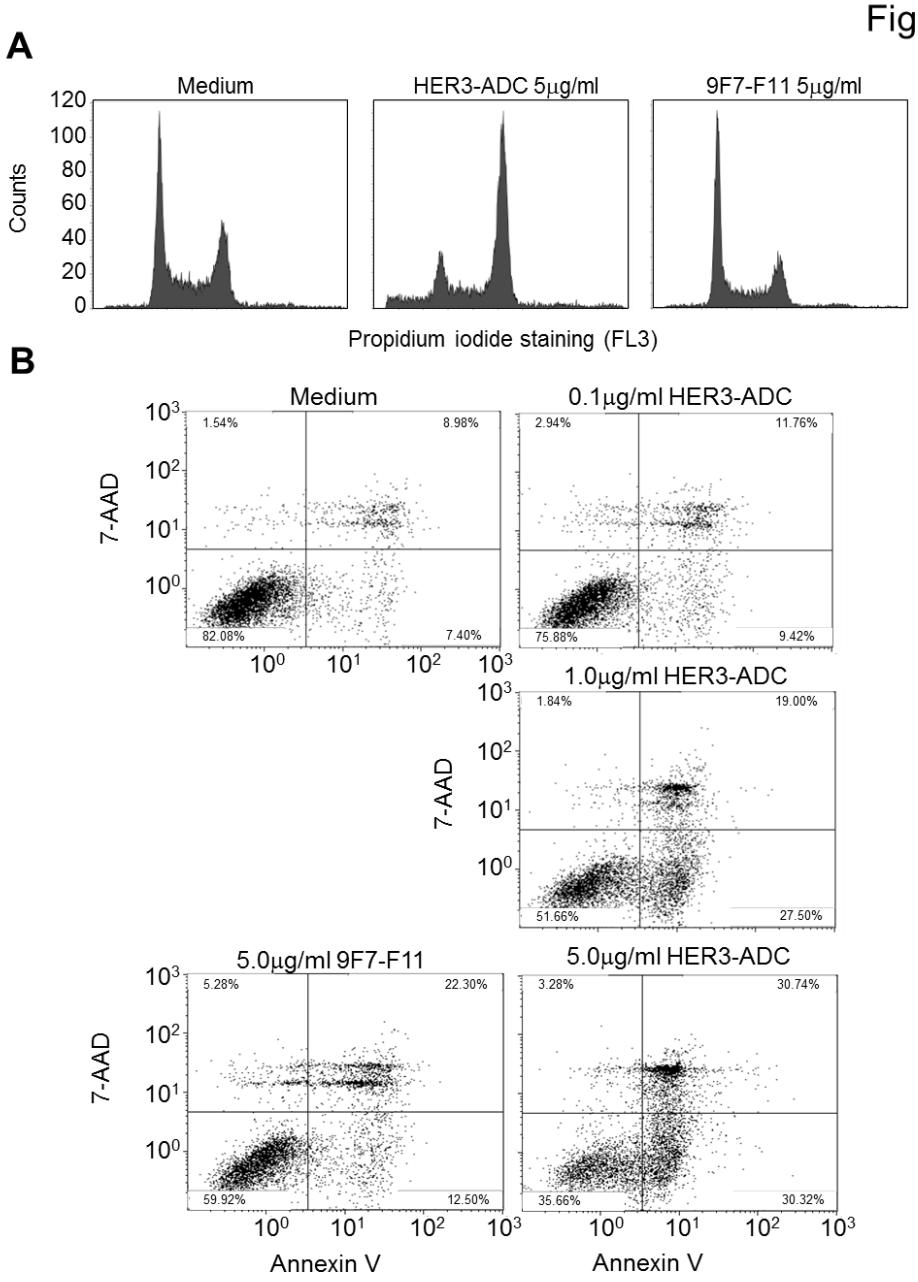

Supplementary Figure S4. HER3-ADC affects the cell cycle distribution and apoptosis rate of BxPC3 cells. **(A)** Flow cytometry profile of PI-labeled BxPC3 cells incubated with HER3-ADC, 9F7-F11, or medium alone. (B) Flow cytometry analysis of NRG1-stimulated and annexin V/7-ADD-stained BxPC3 cells incubated with HER3-ADC or 9F7-F11 for 48h. Medium: cells were only stimulated with NRG1.

Figure S5

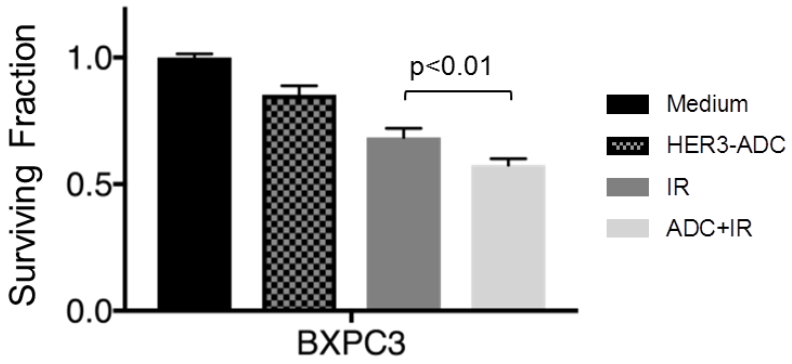

Supplementary Figure S5. HER3-ADC radiosensitizes pancreatic BxPC3 cancer cells. Surviving fraction (i.e., surviving cells in treated samples relative to untreated samples) was measured for BxPC3 cells at day 14 after exposure to 2μg/ml HER3-ADC and/or irradiation (2Gy). The cell surviving fraction of untreated cells (medium) was set to 1.

Figure S6

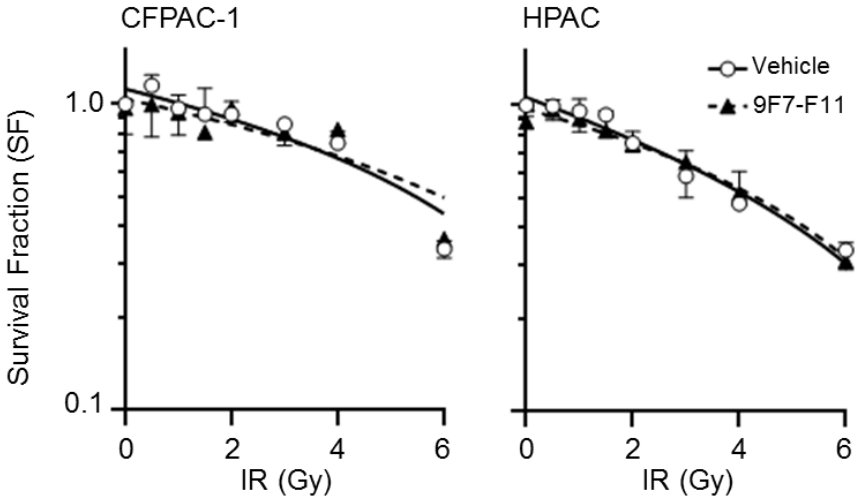

Supplementary Figure S6. Naked 9F7-F11 did not affect clonogenic survival of irradiated pancreatic cancer cells. CFPAC-1 and HPAC cells were treated with 100μg/ml naked 9F7-F11 or vehicle during 4h before irradiation. Data are plotted as mean surviving fraction ± SD.

Figure S7

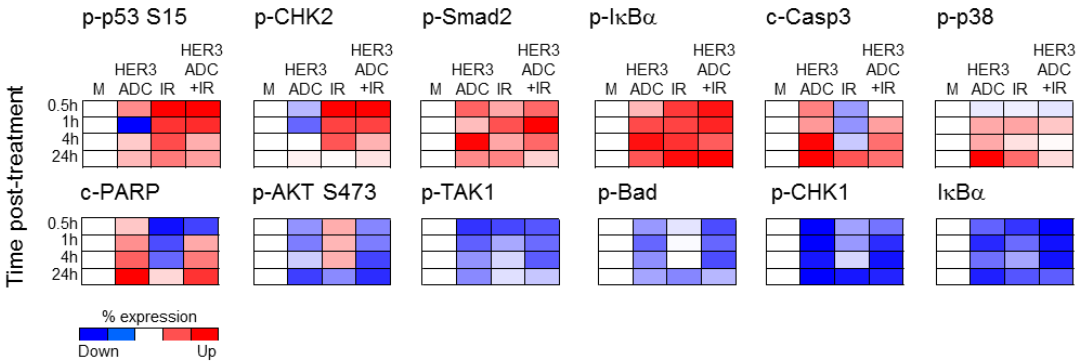

Supplementary Figure S7. HER3-ADC inhibits radiation-induced survival pathways, and favors apoptotic signaling. Temporal expression changes of p-p53, p-CHK2, p-SMAD2, p-IkBa, c-Casp-3, p-p38 and c-PARP (mostly upregulated), and p-AKT, p-TAK1, p-BAD, p-CHK1 and IkBa (downregulated) in the different experimental conditions described in Fig.6A. M: BxPC3 cells stimulated only with NRG1.